DOI: 10.48011/asba.v2i1.970

# Iris image quality on enhanced biometric recognition performance

**Rodrigo N. França*. David A. Ribeiro**. Renata L. Rosa*. Demostenes Z. Rodriguez***

**Federal University of Lavras, DCC*, DAT**, Campus Lavras, Brazil (Tel:(35)3829-1675; e-mail: nani77@gmail.com, david.augusto.ribeiro@gmail.com, rrosa77@gmail.com, demostenes.zegarra@ufla.br).*

**Abstract:** Nowadays, recognition patterns play an important role in several applications, in which the iris recognition is widely developed in authentication systems today. For such systems models, it is necessary to use as input high quality images, which will reduce possible recognition errors. Thus, this article develops experimental tests to study the image quality on the performance of the iris recognition, using different quality metrics. Thus, experiments are conducted with different iris images and applying the Hamming distance algorithm as reference measurement to accept or denied an user authentication. To this end the OSIRIS platform was used in the tests, because it permits to calculate the Hamming Distance between two binary codes. Based on the results obtained in the tests using different metrics, can be inferred that the image quality has a considerable impact on the performance of an iris recognition system. Therefore, the image capture process is an important step.

**Resumo:** Atualmente, os padrões de reconhecimento desempenham um papel importante em diversas aplicações, nas quais o reconhecimento da íris é amplamente desenvolvido nos sistemas de autenticação atuais. Para tais modelos de sistemas, é necessário utilizar como entrada imagens de alta qualidade, o que reduzirá possíveis erros de reconhecimento. Assim, este artigo desenvolve testes experimentais para estudar a qualidade da imagem no desempenho do reconhecimento da íris, utilizando diferentes métricas de qualidade. Assim, experimentos são conduzidos com diferentes imagens de íris e aplicando o algoritmo de Distância de Hamming como medida de referência para aceitar ou negar a autenticação do usuário. Para tal, foi utilizada nos testes a plataforma OSIRIS, pois permite calcular a distância de Hamming entre dois códigos binários. Com base nos resultados obtidos nos testes utilizando diferentes métricas, pode-se inferir que a qualidade da imagem tem um impacto considerável no desempenho de um sistema de reconhecimento de íris. Portanto, o processo de captura da imagem é uma etapa importante.

*Keywords*: ISO/IEC 29794-6:2015, Biometric system; Iris recognition; Image quality; Standards.

*Palavras-chaves*: ISO/IEC 29794-6:2015, Sistema biométrico; Reconhecimento de íris; Qualidade de imagem; Padrões.

## 1. INTRODUCTION

Nowadays, there are numerous techniques for user identification and authentication using biometric recognition models, one of which is the iris according to Chang et al. (2009), due to the fact that this parameter is a unique characteristic of each individual, and the advantage of it does not change with aging. Another advantage of this type of biometrics is that it is a non-intrusive method and can be processed reliably.

Methods and systems of biometric authentication against counterfeiting are increasingly required in systems according to Galbally, Marcel and Fierrez (2014), which deals with a new detection method with wide compatibility in current systems through frameworks, maintaining the advantages non-intrusive methods of this type of recognition.

Image quality plays a relevant role in multimedia systems, which are used for many purposes (RODRIGUEZ et al., 2012, 2014, 2016). According to Saavedra, Jimenez and Avila (2007), biometric idenfication deals with the challenge of image quality in acquisition, as image entry can often contain out of focus images, iris covered by eyelashes or eyelids, thus requiring a prior analysis of the image quality before processing.

By default, a biometric iris system can include the following steps in the recognition process: Acquisition - Segmentation - Normalization - Extraction standards - Coding - Recognition, which would culminate in the authentication process of the user. The first stage (acquisition) can be considered the most important of the process, as it is she who will define whether the next stages will be reliable or not, based on factors such as degradation of the image quality, whether due to noise, occlusion or lighting problems, which can define the level of robustness of the system as a whole.

The objective of this research is to study the impact of the image quality of the iris on the performance of a biometric recognition system by means of internationally recognized techniques. The test material is obtained from the CASIA-Iris-Interval-V3 database of CASIA (2017) and the main metrics available in ISO/IEC 29794-6 according to the

ISO/IEC 29794-6: 2015 (2015) documentation. The metrics presented in this standard evaluate the image quality of the iris from two approaches: first considering the quality metrics for a single image and second considering the comparison between two images, in which in this work only nine metrics of the first approach are used.

The parameters used were True Match (TM) and False Non-Match (FNM). The first (TM) is used for cases where the reference value was below the limit after comparing images of authentic individuals, indicating that the recognition was performed correctly. The second (FNM) occurs when the image of the analyzed iris does not correspond incorrectly to a truly corresponding image stored in the database. The objective is to show that the FNM rate is correlated with the quality scores of the input images.

Open source software for iris (OSIRIS 4.1) was used for the experiment and application of the aforementioned techniques, which were worked on by Othman, Bernadette and Garcia (2015), which provide an approach to this research tool useful for the iris recognition community. Developed in C ++ language, it has shown better performance compared to other similar software for biometric iris recognition in the open source scope (PONDER, 2015).

Through the techniques employed, interval values achieved for each metric are obtained and the percentage of images that are below the reference value are shown. It is important to also present the comparison between images with a series of metrics above the reference values and the parameters (TM and FNM) with the purpose of demonstrating the impact of quality metrics on the proposed model.

This article is divided into the following sections: section 2 describes the theoretical review emphasizing the concepts of biometrics, addresses the steps involved in biometric recognition of an iris and a brief review of the main quality metrics that can be applied to an iris image based on in ISO/IEC 29794-6: 2015. Section 3 presents the proposed research methodology. Section 4 presents the results achieved with the implementation of quality metrics in a specific database. Finally, in Section 5 the conclusions are presented.

## 2. THEORETICAL REVIEW

The use of biometric identification systems for people based on their physical and behavioral characteristics, is a very old technique according to the National Science and Technology Council (NSTC) Subcommittee of SBBCT (2006). One of the most basic and ancient forms of biometric recognition was through the face, so people were identified as known (family members) and unknown (non-family members). Behavioral characteristics were also used, such as the voice and patterns of human locomotion. The first system of capturing images of the palms for biometric identification proposed was in India in 1858 according to William Hershel (1916) and a few years later Galton (1892) presented a study on the recognition of fingerprints (MARANA; JAIN, 2005). Today, the diversity of biometric systems has expanded, including those based on face, hand and ear geometry, characteristics of the voice, odor, retina, iris and DNA.

Biometric systems are classified into unimodal and multimodal. Unimodal systems use information extracted from a single source and multimodal systems use information from two or more sources (COSTA et al., 2015). It should be noted that the present work brings a unimodal approach based on the evaluation of identification under aspects of the characteristics of the texture of the iris. Table 1 shows a comparison between the main current biometric techniques and the level of each one (Low – Medium (average) - High) in relation to the following aspects: universality, distinction (oneness), permanence (stay), collectability (data collect), performance, acceptability and imposture.

**Table 1. Comparison of some techniques of biometrics.**

| FEATURE | DNA | EAR | FACE | FINGERPRINT | IRIS |
|---|---|---|---|---|---|
| UNIVERSALITY | HIGH | AVER. | HIGH | AVER. | HIGH |
| ONENESS | HIGH | AVER. | LOW | HIGH | HIGH |
| STAY | HIGH | HIGH | AVER. | HIGH | HIGH |
| DATA COLLECT | LOW | AVER. | HIGH | AVER. | AVER. |
| PERFORMANCE | HIGH | AVER. | LOW | HIGH | HIGH |
| ACCEPTABILITY | LOW | HIGH | HIGH | AVER. | LOW |
| IMPOSTURE | LOW | AVER. | HIGH | AVER. | LOW |

The first idea of using iris texture as a method of authentication was proposed by ophthalmologist Frank Burch (1936) and documented by James Daggarts (1949). However, the proposal to automatically identify an individual through the characteristics of the iris was made official and patented only in 1987 by Aran and Leonard (FLOM; SAFIR, 1987). In 1993, John Daugman developed an algorithm capable of recognizing an individual by analyzing the texture of the iris (DAUGMAN, 1993). The method is based on the *Wavelet transform* and a *Gabor filter* is represented by a sequence of 256 bytes, this binary representation is called *IrisCode*. The obtained binary codes are compared by a simple computational logic operation. The OSIRISV4.1 presents the segmentation process based on the *Viterbi algorithm*. The software works with the following four steps (modules): segmentation, normalization, coding and recognition (SUTRA; DORIZZI, 2012). Are they:

**Segmentation**: In Figure 1, the software tries to accurately identify the contours of the iris, known as the inner region (pupil/iris) and outer region (iris/sclera) to classify pixels into two classes: iris and non-iris. As a result, a binary mask, pixels with a value of 1 for iris regions and 0 for non-iris regions is created. In addition, two contour regions (pupil and iris) are generated. In Sutra and Dorizzi (2012) the artifacts generated in the segmentation stage are presented.

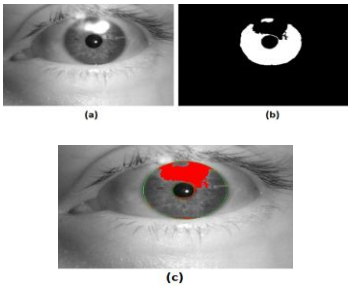


Fig. 1 Segmentation process generated by OSIRIS v4.1. (a) Original image; (b) Binary mask to represent an interest area; (c) Iris segmentation.

**Normalization**: Figure 2 involves the transformation of the iris area into an invariant image size, applying the method proposed by Daugman: *Rubber-sheet-model*. This step is also applied to the generated mask (SUTRA; DORIZZI, 2012).

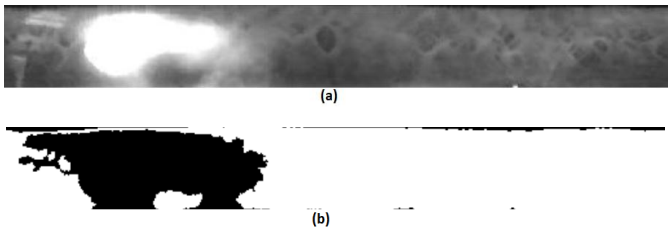


Fig. 2 Normalized images generated by OSIRIS v4.1. (a) The normalized iris region.; (b) Standard binary mask - same iris region, but highlighting occlusion/noise in black regions.

**Coding**: In Figure 3, the iris texture is extracted from the application of a *Gabor filter* bank, resulting in an iris model. OSIRIS allows the customization of these filters (orientation and resolution). The phases of the *Gabor filters* are then encoded in 2-byte iris code and the IrisCode is generated. In this case, a filter bank composed of three *Gabor filters* (generating 6 different resolutions) was applied. Each *Gabor filter* has real and imaginary parts in its representation, which are used to form the iris code.

Fig. 3 Code/iris template (IrisCode) generated by OSIRIS v4.1. Othman, Dorizzi and Garcia-Salicetti (2015).

**Recognition** (matching): In Figure 4, the recognition step compares two iris codes applying the *Hamming Distance* (HD) between their binary codes represented by the points of interest, the selection of which is customizable. The masks generated in the segmentation module are used to identify and ignore the noise in the original images, improving the accuracy of the results.

Figure 4 represents the recognition steps, in which HD is obtained between two different iris codes. At this stage, the application of points of interest is grouped with the binary masks of each of the images, and then an *XOR* operation is applied to the iris codes along the two masks and the predefined application of points of interest, that is, only points of interest that have no noise at all.

Daugman (2004) performed 9.1 million iris comparisons between different individuals and observed that the lowest HD value for the TM parameter was 0.334. Therefore, the comparison between two images of irises that reached values above this limit can be considered as images of different individuals, in turn, values below this value can be considered images of the same individual. However, this specific HD value must be defined according to the characteristics and purposes of the implemented system.

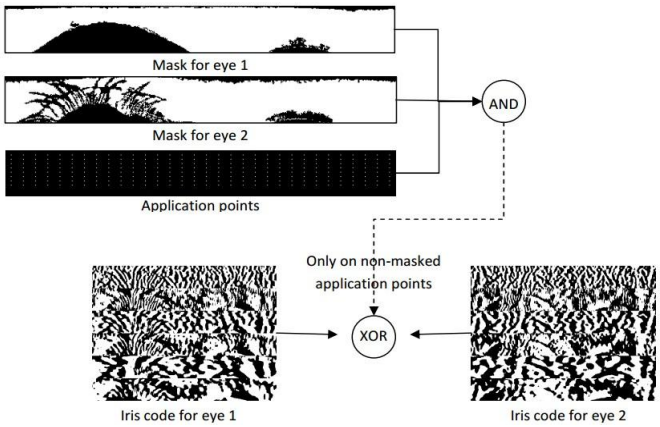


Fig. 4 Representation of the recognition step/OSIRIS matching v4.1. Othman, Dorizzi and Garcia-Salicetti (2015).

The image quality of the iris is approached by different authors in different ways and perspectives (HOFBAUER et al. 2012; KALKA et al. 2006; LI et al. 2011; MAKINANA et al. 2014; REILLO et al. 2012). In turn, the ISO/IEC 29794-6: 2015 standard presents a set of metrics related to the image quality of the iris that must be considered when capturing or processing these images:

**UsableIrisArea**: is the part of the iris not occluded by eyelids, eyelashes, or specular highlights. It is computed as non-occluded portion of the area between two circles that are close to the iris-sclera boundaries and iris-pupil, expressed as percentage. The calculation is performed as follows:

• The approximate boundaries of the iris-sclera and iris-pupil in two circles are defined;

• Set Niris as the amount of pixels between the two circles;

• Set Noccluded as the amount of pixels between the two circles which are occluded by the eyelids, eyelashes, or specular reflections.;

• Then, calculate the UsableIrisArea according to the equation 1:

$$UsableIrisArea = \left(1 - \frac{N_{occluded}}{N_{iris}}\right) * 100 \quad (1)$$

• An image can be considered acceptable it must have a value of *UsableIrisArea* higher than or equal to 70.

**IrisScleraContrast**: is the image features on the boundary between the iris region and the sclera. A low or insufficient contrast may result in failures in the iris image feature extraction process. The calculation is as follows:

• The approximate boundaries of the iris-sclera and iris-pupil in two circles are defined.

• Normalize the highlighted region to the iris-sclera boundary be at a distance of 1.0;

• Selecting pixels in a ring whose outer radius is 0.9 and whose inner radius extends to the midpoint between the boundaries of the iris, pupil and iris-sclera, which are not blocked by the eyelids or eyelashes. These are called iris pixels;

• Set iris _value (IVisc) as the median of iris pixels;

• Select all pixels that are not occluded by the eyelids, eyelashes, or specular reflections in a ring inner radius and outer radius of 1.1 to 1.2. These are called sclera pixels;

• Set sclera value (SV) as the median of the sclera pixels and then calculate the IrisScleraCont according to the equation 2:

$$IrisScleraCont = \begin{cases} 0 \; if \; PV \geq IV_{isc} \; or \; PV \geq SV \\ \frac{|SV - IV_{isc}|}{SV + IV_{isc} - 2 * PV}.100, \quad otherwise \end{cases} \tag{2}$$

Where: PV (pupil value) is defined in the next subsection. The reference value for an acceptable image quality has to be greater than 5.

**IrisPupilContrast**: is the image features on the boundary between the iris and pupil region. Also, the existence of sufficient contrast for an acceptable iris image segmentation is necessary. A low or insufficient contrast may result in failures in the iris image feature extraction process. The calculation is as follows:

• Define the approximate boundaries of the iris, pupil and iris-sclera in two rounds;

• Normalize the boundary region of the iris-pupil in a distance of 1.0;

• Select the pixels within a circle of radius 0.8 that are not blocked by the eyelids, eyelashes or boundary of contact lenses. These are called pupil pixels;

• Set pupil value (PV) as the median of the pupil pixels;

• Select all pixels that are not occluded by the eyelids, eyelashes, or specular reflections and in which a ring is 1.1 inner radius and outer radius extends to the midpoint between the boundaries of the iris-pupil and iris-sclera. These points are called iris pixels;

• Set iris value (IVipc) as the median of the pixels of the iris;

• Calculate the first weberRatio and then find the IrisPupilContrast as following equations 3 and 4:

$$weberRatio = \frac{|IV_{ipc} - PV|}{(20 + PV)} \tag{3}$$

$$IrisPupilContrast = \left(\frac{weberRatio}{0.75 + weberRatio}\right).100 \tag{4}$$

The reference value for an acceptable image quality must be greater than or equal to 30.

**Pupil Boundary Circularity** (PupilBC): It is the circularity of the iris-pupil boundary. It must be measured by the total modulus (sum of squared coefficients) of the real and imaginary parts of the Fourier series expansion on the pupil boundary, depending on the radius of the angle around the center. The PupilBoundaryCircularity equation can be found from C which are the discrete coefficients of Fourier derived from the sequence of rθ:

$$C_k = \sum_{\theta=0}^{N-1} r_\theta e^{-2\pi i k\theta/N} \tag{5}$$

$$PupilBC = \max\left(0{,}100 - \frac{1}{N}\sum_{k=1}^{M-1}\|C_k\|^2\right) \tag{6}$$

The reference value is 100 for a circle and it is [0,100] to other forms.

**Gray scale utilization**: checks the values of pixels of an iris image to show a scattering intensity values in the image of the iris. A useful iris image should have a dynamic range of 256 gray levels, allocating at least 8 bits with a minimum of 6 bits of useful information. In cases of an image underexposed would have very few high intensity pixels. The same problem also occurs to the opposite case, when the image is overexposed. An image with a high score indicates a properly exposed image, with a wide distribution and distributed and intensity values. The calculation must be performed for each gray level i present in the picture, checking the probability of pi. Where pi is the total count of pixels in the gray level i, divided by the total number of pixels in the image. The pixels' histogram entropy (H) in bits, is:

$$H = -\sum_i p_i log_2 p_i \tag{7}$$

The pixels' histogram entropy must be greater than or equal to 6 bits to be considered an image with good quality in this regard.

**IrisRadius**: It is the radius of a circle that approaches the iris-sclera boundary. The measurement is performed on pixels and should be performed after segmentation. The reference value must be at least 80 pixels for the smaller iris-human reported. The average radius the human iris is 5.9 millimeters with a strip 5.1 to 6.5 millimeters.

**PupilIrisRatio**: Represents the degree of pupil dilation, whether it is contracted or expanded. The benchmark for images with minimum quality must be between 20 and 70.

$$PupilIrisRatio = \left(\frac{PupilRadius}{IrisRadius}\right).100 \tag{8}$$

**Iris Pupil Concentricity** (IPCo): It is the degree to which the center of the pupil and the iris center are in the same location. The concentricity of the iris and the pupil has to be calculated using the Euclidean distance between the centers of the iris and pupil, divided by the iris radius, according to the equation:

$$IPC_o = max\left\{1 - \frac{\sqrt{(X_p - X_i)^2 + (Y_p - Y_i)^2}}{IrisRadius}, 0\right\} .100 \quad (9)$$

Where: (Xi, Yi) and (Xp, Yp) are the center coordinates of the iris and the pupil center, respectively. The reference value must be greater than or equal to 90.

**Margin adequacy**: quantifies the degree of centralization of the iris region in the image relative to the side of the whole image edges. The first calculation is performed to each of the side regions defining: LeftMargin, RightMargin, UpMargin and DownMargin as:

$$LM = \frac{X_{iris} - IrisRadius}{IrisRadius} \quad (10)$$

$$RM = \frac{ImageWidth - (X_{iris} + IrisRadius)}{IrisRadius} \quad (11)$$

$$UM = \frac{Y_{iris} - IrisRadius}{IrisRadius} \quad (12)$$

$$DM = \frac{ImageHeight - (Y_{iris} + IrisRadius)}{IrisRadius} \quad (13)$$

$$LeftMargin = max\left\{0, \min\left\{1, \frac{LM}{0.6}\right\}\right\} \quad (14)$$

$$RightMargin = max\left\{0, \min\left\{1, \frac{RM}{0.6}\right\}\right\} \quad (15)$$

$$UpMargin = max\left\{0, \min\left\{1, \frac{UM}{0.2}\right\}\right\} \quad (16)$$

$$DownMargin = max\left\{0, \min\left\{1, \frac{DM}{0.2}\right\}\right\} \quad (17)$$

Finally, the MarginAdequacy (MAdeq) calculation is expressed by the following equation:

$$MAdeq = 100 . min\begin{Bmatrix} LeftMargin, & RightMargin \\ UpMargin, & DownMargin \end{Bmatrix} \quad (18)$$

The reference value, for this quality metric, must be greater than 80.

**Sharpness**: Measures the focus degree on the image. The sharpness is measured by the power spectrum after filtering with a Laplacian of Gaussian operator. The Gaussian standard deviation is 1.4. The steps to perform the Sharpness calculation are:

• A convolution filter with kernel F is defined:

$$F = \begin{bmatrix} +00 & +01 & +01 & +02 & +02 & +02 & +01 & +01 & +00 \\ +01 & +02 & +04 & +05 & +05 & +05 & +04 & +02 & +01 \\ +01 & +04 & +05 & +03 & +00 & +03 & +05 & +04 & +01 \\ +02 & +05 & +03 & -12 & -24 & -12 & +03 & +05 & +02 \\ +02 & +05 & +00 & -24 & -40 & -24 & +00 & +05 & +02 \\ +02 & +05 & +03 & -12 & -24 & -12 & +03 & +05 & +02 \\ +01 & +04 & +05 & +03 & +00 & +03 & +05 & +04 & +01 \\ +01 & +02 & +04 & +05 & +05 & +05 & +04 & +02 & +01 \\ +00 & +01 & +01 & +02 & +02 & +02 & +01 & +01 & +00 \end{bmatrix}$$

• If I(x,y) is an image, then the weighted sum of I(x,y) according to F is calculated for each fourth row and column position I(x, y). As $I_F$(x, y) representing the filtered output, then:

$$I_F(x,y) = \sum_{i=-4}^{4} \sum_{j=-4}^{4} I(x+i, y+j) F(i+5, j+5) \quad (19)$$

$$\forall x \in [1,5, \dots, \omega], y \in [1,5, \dots, h]$$

Where ω and h are width and height of I(x,y), respectively.

• Then, calculate the square sum (squareSum) $I_F$(x,y):

$$squareSum = \sum_{\forall x,y \in I_F(x,y)} I_{F(x,y)^2} \quad (20)$$

• Then, calculates the power in the $I_F$(x,y):

$$power = \frac{sumSquare}{\omega_F \, . \, h_F} \quad (21)$$

Where $\omega_F$ and $h_F$ are the width and height of $I_F$(x,y), respectively. Finally, using the equation below sharpness value is calculated:

$$Sharpness = 100 . \frac{power^2}{power^2 + c^2} \quad (22)$$

Where the value of c, empirically chosen, was of 1800000. Table 2 summarizes the metrics presented and their reference values (RV).

## 3. MATERIAL AND METHODS

Due to the large amount of information to be processed in the model, a framework was developed that considers the implementation of metrics for assessing image quality, communication with OSIRIS, and a database to classify the result using specific criteria.

**Table 2. Metrics iris image quality and their reference values.**

| COD. | QUALITY METRICS | REFERENCE VALUES (RV) (IDEALS) |
|---|---|---|
| Q1 | Usable iris area | ≥ 70 |
| Q2 | Iris-sclera contrast | >5 |
| Q3 | Iris-pupil contrast | ≥ 30 |
| Q4 | Pupil boundary circularity | 100 to a circle and [0, 100] to other forms |
| Q5 | Gray scale utilization | ≥ 6*bits* |
| Q6 | Iris radius | ≥ 80*pixels* |
| Q7 | Pupil dilation | Between 20 and 70 |
| Q8 | Iris pupil concentricity | ≥ 90 |
| Q9 | Margin adequacy | >80 |
| Q10 | Sharpness | Undefined |

Several public databases of iris images were analyzed, and CASIA-Iris-Interval-V3 was selected for the tests, as it is a database well known in the literature and easily accessible. This database provides images with different levels of quality obtained in different sessions of 249 individuals, totaling 2639 images. After analyzing some biometric iris recognition software, which provide the source code for simulations and

tests (MASEK, 2009), and according to an extensive study by Ponder (2015) OSIRIS was chosen for the job due to factors such as open source software, accurate results and low processing time compared to other software in the literature.

All 2639 images were processed in OSIRIS, with the creation of new data from the image input, namely: CircleParameters ('.txt' file with information on the pupil and iris location points), IrisCode (binary images containing the generated templates), Masks (binary images highlighting only the area of interest, after removing possible occlusions and noise), NormalizedImages (original images after normalization by the *Rubber-Sheet-Model* method proposed by Daugman), NormalizedMask (images of masks, but normalized), **Scores** ('.txt' file containing the names of the compared images and the HD between them) and SegmentedImages (original image highlighting circular regions of the iris/pupil and regions of occlusion).

From the moment the OSIRIS was processed, metrics for evaluating the quality of the iris image presented in ISO/IEC 27974-6: 2015 were implemented in the MATLAB software, with the proposal of mapping the study of the database from these metrics. Only the Sharpness metric was not considered, since a reference value for this metric is not suggested. Thus, all 2639 images from the CASIA-Iris-Interval-V3 database were evaluated by the nine selected metrics. To assist in the analysis of the results and quality indexes obtained, all data generated by MATLAB and OSIRIS were integrated into a system/database developed in Microsoft Access software, in which filters can be applied and the quality criteria evaluated can be ordered.

## 4. RESULTS AND DISCUSSION

The fact of creating an integrated database containing the data generated by OSIRIS with 9 quality metrics (Q1 - Q9), allowed an analysis of the set of images per metric. Table 3 shows the statistics (minimum (MIN), maximum (MAX) and average (AVERAGE)) for each of the metrics evaluated among the 2639 images used as test material. The graphs for each of the quality metrics used are presented in Figures 5 to 13. It is possible to identify in these figures some highlighted regions, representing the images above the *Reference Values* (RV), in which they achieved the minimum required quality score. Another way to analyze the results is presented in Table 4, in which the images were grouped according to the number of metrics above the RV, noting that approximately 75% of the analyzed images (1951 images) reached at least eight of the nine metrics quality above RV.

By the observations, 15 images (0.57%) among the 2,639, ad five quality metrics above the RV. Figures 7, 10 and 11 (Q3, Q6 and Q7 respectively) show that the reference values of these metrics were reached by almost all images processed, so a review of these reference values can be studied in order to adjust them for more optimized results. Figure 14 presents an overview of the metrics used separately, in which it can be seen that only the metric Q9 (Adequacy of the margin) is below the other metrics (20%). This fact is probably due to the fact that when these images were captured, he was not concerned with centralizing the object (iris).

**Table 3. Information quality metrics with applied statistics in the database under study.**

| COD. | QUALITY METRICS | MIN | MAX | AVERAGE |
|---|---|---|---|---|
| **Q1** | Usable iris area | 17.827 | 98.669 | 79.444 |
| **Q2** | Iris-sclera contrast | 0 | 41.567 | 13,286 |
| **Q3** | Iris-pupil contrast | 28.235 | 78.465 | 65.123 |
| **Q4** | Pupil boundary circularity | 88.788 | 100.734 | 98.664 |
| **Q5** | Gray scale utilization | 4,861 | 7.7824 | 7.100 |
| **Q6** | Iris radius | 77.993 | 124.988 | 104.129 |
| **Q7** | Pupil dilation | 22.220 | 61.428 | 39.077 |
| **Q8** | Iris pupil concentricity | 78.876 | 99.970 | 94.080 |
| **Q9** | Margin adequacy | 0 | 100 | 54.186 |

About 82% of the images are above the RV in the metric Q1 (Iris Usable Area) and Q8 (Iris Pupil Concentricity), indicating that the images below the RV (Q1 ≈ 18%) may have considerable deficiencies in recognition, and the values below of the RV (Q8 ≈ 13%) indicate a possible failure in the segmentation process.

Table 5 shows the comparison between the images of authentic individuals (same individual). In this table, the Quantity of Metrics (QM) indicates that at least one of the compared images obtained QM above the RV, among the 9 applied metrics. Statistical values related to HD and the percentage of cases in which the recognition was performed correctly (TM) and the percentage of cases in which there were failures (FNM) are presented.

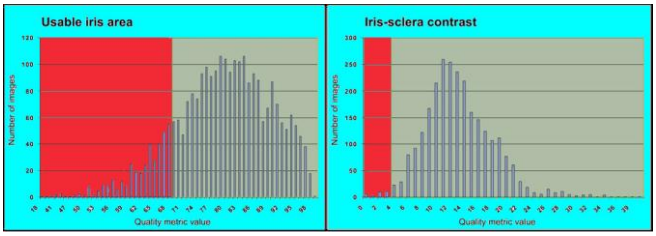


**(a)** **(b)**

Fig. 5 Metric: Q1 - Usable i. area (RV: ≥ 70). (a)

Fig. 6 Metric: Q2 - Iris-s. contrast (RV: > 5). (b)

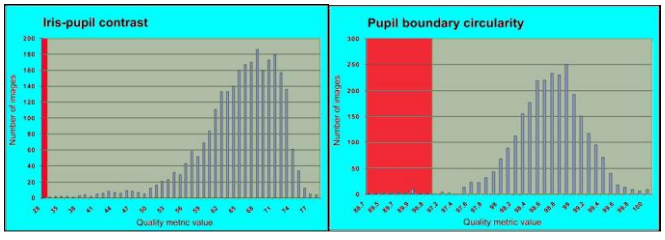


**(c)** **(d)**

Fig. 7 Metric: Q3 - Iris-pupil contrast (RV: ≥ 30). (c)

Fig. 8 Metric: Q4 - Pupil b. circularity (RV: ≥ 97). (d)

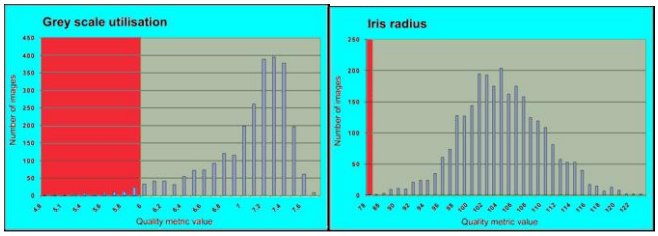


**(e)** **(f)**

Fig. 9 Metric: Q5 - Gray s. utilization (RV: ≥ 6 bits). (e)

Fig. 10 Metric: Q6 - Iris radius (RV: ≥ 80 pixels). (f)

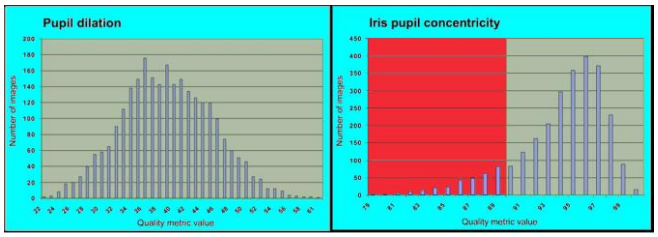


**(g)** **(h)**

Fig. 11 Metric: Q7 - Pupil dilation (RV: 20 to 70). (g)

Fig. 12 Metric: Q8 - Iris p. concentricity (RV: ≥ 90). (h)

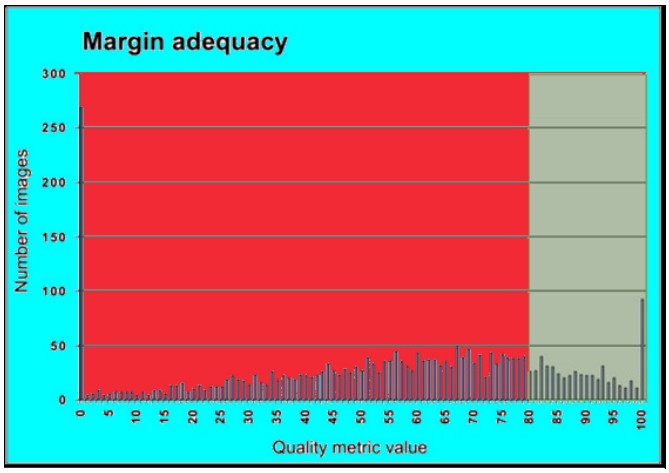


**(i)**

Fig. 13 Metric: Q9 – Margin adequacy (RV: > 80). (i)

**Table 4. Images number grouped by quality metrics above the reference value..**

| NUMBER OF METRICS ABOVE THE REFERENCE VALUE. (TOTAL: 9 METRICS ANALYZED) | NUMBER OF IMAGES | % IMAGES |
|---|---|---|
| 9/9 | 384 | 14.55 |
| 8/9 | 1567 | 59.38 |
| 7/9 | 548 | 20.77 |
| 6/9 | 125 | 4.74 |
| 5/9 | 15 | 0.57 |
| TOTAL | 2639 | 100 |

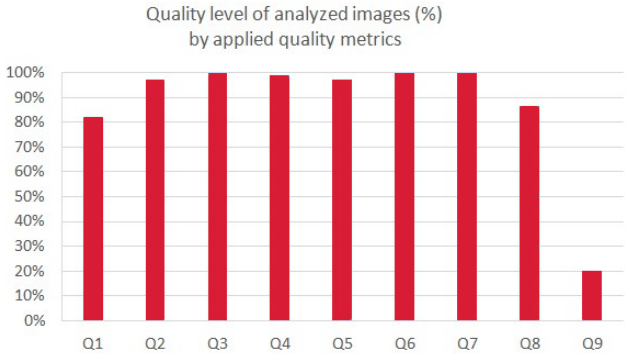


Fig. 14 Overall assessment of the quality level of the analyzed images.

**Table 5. Images number grouped by quality metrics above the reference value.**

| QM | AVERAGE HD | MINIMUM HD | MAXIMUM HD | TM (%) | FNM (%) |
|---|---|---|---|---|---|
| 9 | 0.2447 | 0.0984 | 0.4904 | 97.38% | 2.62% |
| 8 | 0.2429 | 0.0889 | 0.4904 | 96.52% | 3.48% |
| 7 | 0.2528 | 0.1024 | 0.4904 | 94.48% | 5.52% |
| 6 | 0.2678 | 0.0889 | 0.5085 | 89.61% | 10.39% |
| 5 | 0.2782 | 0.1434 | 0.4358 | 91.03% | 8.97% |

As expected, the results presented in Table 5 prove that if the quality of the images increases, the rate of NMF is reduced, therefore the overall performance of the biometric iris recognition system improves. In the case of QM = 9, only a few images are categorized as FNM, and after visual examination of these cases, it was found that the images compared are different, as one of the images had a rotation angle in relation to the other. Which shows an important factor in relation to international metrics in which the current set of image quality is unaware of this type of error in the image acquisition process.

## 5. CONCLUSION

It is important for the performance of biometric iris recognition systems to use images with a minimum quality limitation under efficient metrics parameters, as the incidence of failures is reduced with increasing image quality. Images with problems such as occlusion, poor lighting and angulation impair the recognition result, requiring automatic identification and subsequent exclusion of these images with low quality index. The experimental results show that the set of quality metrics of the ISO / IEC 29794-6: 2015 standard can be improved, including a new metric related to the rotation of the iris. Through the analysis of the VR of some metrics and their refinement, it will soon be possible to achieve systems with greater performance.

REFERENCES


CASIA Iris-Interval Databases. Accessed: Aug. 2017. [Online]. Available: http://biometrics.idealtest.org

Chang, C.P., Lee, J.C., Su, Y., Huang P.S., and Tu, T.M., "Using empirical mode decomposition for iris recognition," Computer Standards Interfaces., vol. 31, no. 4, pp. 729–739, 2009.

Costa, D.M.M., Passos, H., Peres, S.M., and Lima, C.A.M., "A comparative study of feature level fusion strategies for multimodal biometric systems based on face and iris," in: Proc. of the Conference on Brazilian Symposium on Information Systems. Brazilian Computer Society, Porto Alegre, Brazil, no. 30, pp. 219–226, 2015.

Daugman, J.G., "High confidence visual recognition of persons by a test of statistical independence," in: IEEE Transactions Pattern Anal. Mach. Intell., Washington, DC, USA, vol. 15, no. 11, pp. 1148–1161, 1993.

Daugman, J.G., "How iris recognition works," in: IEEE Transactions on Circuits and Systems for Video Technology., vol. 14, no. 1, pp. 21–30, 2004.

Flom, L., and Safir, A., "Iris recognition system," Feb. 1987.

Galbally, J., Marcel, S., and Fierrez, J., "Quality measurements for iris images in biometrics," IEEE Transactions on image processing., vol. 23, no. 2, Feb. 2014.

Galton, F., in: Finger prints. MacMillan and Company, London, UK, 1892.

Hofbauer, H., Rathgeb, C., Uhl, A., and Wild, P., "Iris Recognition in Image Domain: Quality-Metric Based Comparators," Springer Berlin Heidelberg. Berlin, Heidelberg, pp. 1–10, 2012.

ISO/IEC 29794-6: 2015, Information technology: Biometric sample quality - part 6: Iris image data. [Online]. Available: https://www.iso.org/standard/54066

Kalka, N.D., Zuo, J., Schmid, N.A., and Cukic, B., "Image quality assessment for iris biometric," in: Proc. Defense and Security Symposium. Orlando, FL, USA. vol. 6202, pp. 62020D-1–62020D–11, 2006.

Li, X., Sun, Z., and Tan, T., "Comprehensive assessment of iris image quality," in: IEEE International Conference on Image Processing. Brussels, Belgium, pp. 3117–3120, 2011.

Makinana, S., Malumedzha T., and Nelwamondo, F.V., "Iris image quality assessment based on quality parameters," in: Asian Conference on Intelligent Information and Database Systems. Springer-Verlag, New York, Bangkok, Thailand. vol. 8397, pp. 571–580, 2014.

Marana, N., and Jain, A.K., "Ridge-based fingerprint matching using hough transform," in: Brazilian Symposium on Computer Graphics and Image Processing (SIBGRAPI). Natal, RN, Brazil, pp. 112–119, 2005.

Masek, L., "Recognition of Human Iris Patterns for Biometric Identification," Bachelor of Engineering, 2009. [Online]. Available: https://www.peterkovesi.com/studentprojects/libor

Othman, N., Bernadette, B., and Garcia-Salicetti, S., "Osiris: An open source iris recognition software," in: Pattern Recognition Letters., vol. 82, no. 1, pp. 124–131, 2015.

Ponder, C.J., "A generic computer platform for efficient iris recognition," Ph.D. thesis, University of Glasgow., 2015.

Reillo, R.S., Moreno, R.A., Saavedra, B.F., and Kwon, Y.B., "Standardized system for automatic remote evaluation of biometric algorithms," Computer Standards Interfaces. vol. 34, no. 5, pp. 413 – 425, 2012.

S. B. B. Committee on Technology, in: National Science and Technology Council., USA, 2006.

Saavedra, B. F., Jimenez, J. L. and Avila, C. S., "Quality Measurements for Iris Images in Biometrics," in EUROCON 2007 The International Conference on Computer as a Tool. Sep. 2007.

Sutra, G., Garcia-Salicetti, S., and Dorizzi, B., "The viterbi algorithm at different resolutions for enhanced iris segmentation," in: IAPR International Conference on Biometrics (ICB)., New Delhi, India, pp. 310–316, 2012.

Sutra, G., and Dorizzi, B., "Iris osiris v4.1," in telecom sud paris. 2012 [Online]. Available: http://svnext.it-sudparis.eu/svnview2-eph/ref_syst/Iris_ Osiris_v4.1

Rodriguez, D. Z., Abrahao J., Begazo D. C., Rosa R. L. and Bressan G., "Quality metric to assess video streaming service over TCP considering temporal location of pauses," in IEEE Transactions on Consumer Electronics, vol. 58, no. 3, pp. 985-992, August 2012.

Rodriguez, D. Z, Rosa R. L, Costa Alfaia E., Abrahão J. and Bressan G "Video quality assessment in video streaming services considering user preference for video content," in IEEE Transactions on Consumer Electronics, vol. 60, no. 3, pp. 436-444, Aug. 2014,

Rodriguez, D. Z, Rosa R. L, Costa Alfaia E., Abrahão J. and Bressan G., "Video Quality Metric for Streaming Service Using DASH Standard," in IEEE Transactions on Broadcasting, vol. 62, no. 3, pp. 628-639, Sept. 2016,